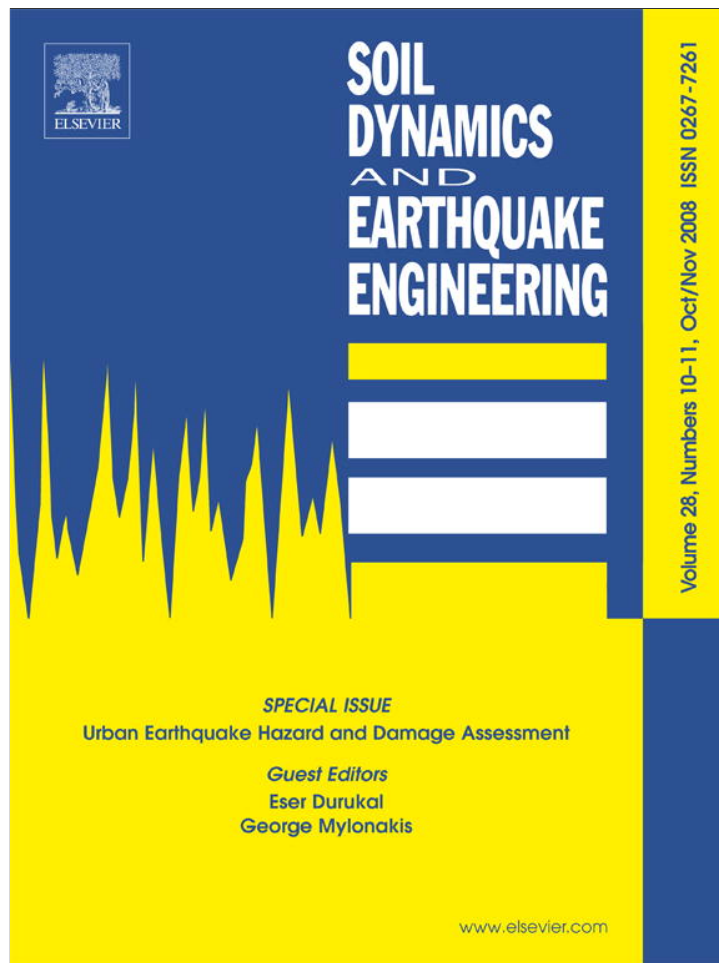


Provided for non-commercial research and education use.
Not for reproduction, distribution or commercial use.



This article appeared in a journal published by Elsevier. The attached copy is furnished to the author for internal non-commercial research and education use, including for instruction at the authors institution and sharing with colleagues.

Other uses, including reproduction and distribution, or selling or licensing copies, or posting to personal, institutional or third party websites are prohibited.

In most cases authors are permitted to post their version of the article (e.g. in Word or Tex form) to their personal website or institutional repository. Authors requiring further information regarding Elsevier's archiving and manuscript policies are encouraged to visit:

<http://www.elsevier.com/copyright>



Seismic hazard and risk in Shanghai and estimation of expected building damage

Stephen W. Cole*, Yebang Xu, Paul W. Burton

School of Environmental Sciences, University of East Anglia, Norwich NR4 7TJ, UK

Received 13 October 2006; received in revised form 4 July 2007; accepted 11 October 2007

Abstract

The People's Republic of China is in the process of rapid demographic, economic and urban change including nationwide engineering and building construction at an unprecedented scale. The mega-city of Shanghai is at the centre of China's modernisation. Rapid urbanisation and building growth have increased the exposure of people and property to natural disasters. The seismic hazard of Shanghai and its vicinity is presented from a seismogenic free-zone methodology. A PGA value of 49 cm s^{-2} and a maximum intensity value of VII for the Chinese Seismic Intensity Scale (a scale similar to the Modified Mercalli) for a 99% probability of non-exceedance in 50 years are determined for Shanghai city. The potential building damage for three independent districts of the city centre named Putuo, Nanjing Road and Pudong are calculated using damage vulnerability matrices. It is found that old civil houses of brick and timber are the most vulnerable buildings with potentially a mean probability value of 7.4% of this building structure type exhibiting the highest damage grade at intensity VII.

Crown Copyright © 2007 Published by Elsevier Ltd. All rights reserved.

Keywords: Shanghai; Seismic hazard; Seismic risk; Building damage

1. Introduction

Shanghai is one of the largest cities of China with 13.4 million inhabitants and is considered as the country's leading economic, commercial and business centre. Rapid urbanisation and worker migration has increased demand on the city's infrastructure and resources. Its rapid growth as a megacity is a result of unprecedented building growth. From 1991 to 2003 Shanghai invested a total of more than 479.88 billion Yuan (\$US 8 billion) in urban construction projects [1] a result of government and economic reforms. It currently has the world's largest cargo port and longest sea-bridge. In 2010 it is venue to the World Expo, an opportunity to demonstrate and consolidate itself as a modern day 21st century city. However, previous inadequate land planning and an increased wealth gap have resulted in a city of contrasting status evident with the juxtaposition of skyscrapers and poorly maintained housing. The increased exposure and vulnerability of

populations to natural disasters is hastening the need to determine potential losses for the use of urban and emergency planners, builders, engineers and the insurance sector. This paper looks at potential building damage for an earthquake event for three districts of Shanghai city that characterise different aspects of its building stock following an assessment of the seismic hazard in the urban area and its vicinity.

2. Location and tectonic setting

Situated on the eastern seaboard of China, Shanghai city is located at 31.14°N , 121.29°E . The city is part of Shanghai municipality which borders the provinces of Jiangsu to the north-west and Zhejiang to the south-west (Fig. 1). Directly north lies the mouth of the Yangtze River and directly south is Hangzhou Gulf bay. To the east lies the northern section of the East China Sea (Fig. 1). Covering 6340 km^2 [2], Shanghai municipality is divided into 10 main districts. Within the city centre Puxi and Pudong New Area districts lie west and east of the

*Corresponding author. Tel.: +44 1603 593990; fax: +44 1603 591327.
E-mail address: s.cole@uea.ac.uk (S.W. Cole).

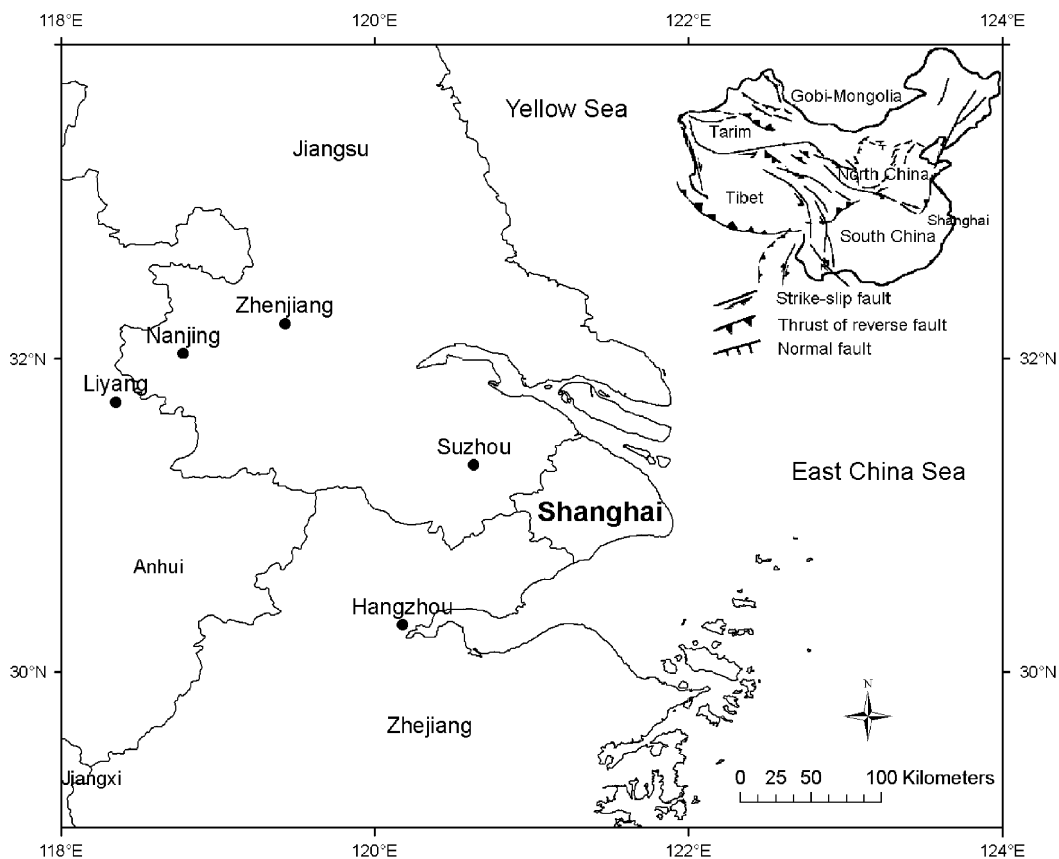


Fig. 1. Location of Shanghai, neighbouring cities and relation to China tectonics.

Huangpu River, respectively. Shanghai municipality is located within the Yangtze alluvial river plain, which was laid down in the last 5000 years, and the lacustrine plain of Taihu Lake. Geological sediments are generally Quaternary apart from isolated Jurassic outcrops to the west of the municipality [2]. This area of eastern China is part of the South China block, a stable continental region that is tectonically rigid, thermally cold and with no major tectonic activity since the early Mesozoic [3].

3. Earthquake catalogue and seismicity

A comprehensive earthquake catalogue was obtained from the Shanghai Seismological Bureau (SSB). It provides details regarding time of earthquake in the year, month, and day format. Also tabulated is earthquake location in latitude and longitude coordinates, focal depth in km, and earthquake magnitude expressed using surface-wave magnitude M_s . The initial catalogue covers the period from 237 to 2002 AD with a total of 1169 records. An updated catalogue has been added to the original catalogue so that the working catalogue is from 237 to 2004 AD with a total of 1200 events. It tabulates earthquake data for Shanghai municipality, Jiangsu and Zhejiang provinces together with seismic events in Anhui province to the west and also off-shore earthquakes under the Yellow and East China seas.

The catalogue is divided into three recording periods: from 237 to 1900, 1900 to 1970, and 1970 to 2004. From 237 to 1900 historical records are documented. In terms of location, certain historical earthquakes would have been attributed to the capital of the district of that time, e.g. Nanjing. Earthquakes described as “small” were assigned magnitude 3.0. Instrumental readings from Chinese seismoscopes were recorded from 1900 and from 1970 to the present day a detailed local network of seismic recording stations is established which gives greater accuracy on earthquake events including more specific focal depth data. There are 1200 recorded earthquakes for the area of 27–35°N by 115–125°E of magnitude 3.0 or greater since 237 AD and 394 (32.8%) of these are recorded since 1900. The highest magnitude earthquake is a 7.0 surface-wave magnitude event occurring on 4 August 1846. There are 82 earthquakes above magnitude 5.0. This immediately suggests that the Shanghai area does not experience high hazard magnitude earthquakes. There are more earthquakes greater than 5.0 during the 1800s than 1900s and since 2000 to late 2004 there have been no earthquakes greater than magnitude 4.4 which suggests current low seismicity.

Fig. 2 shows a plot of earthquake epicentres for the whole catalogue in five magnitude ranges of 3–3.9, 4–4.9, 5–5.9, 6–6.9 and 7–7.9. Although early historic records located earthquakes at local provincial capitals and not the

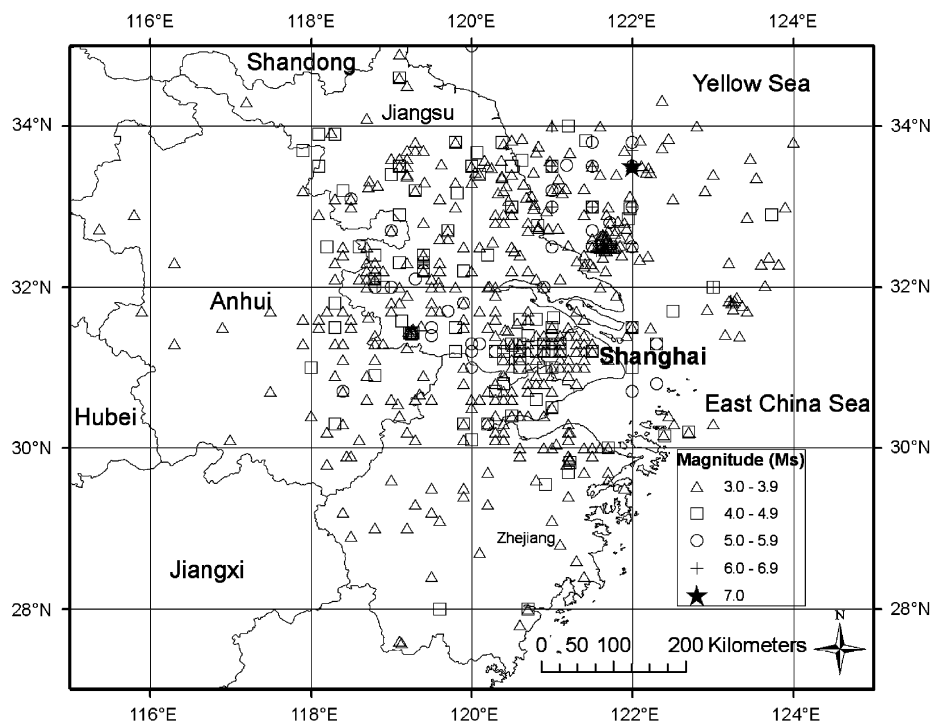


Fig. 2. Seismicity of Shanghai and neighbouring region from 237 to 2004 AD.

exact epicentre locality, certain points can be stated about spatial seismicity in this area. In terms of surface-wave magnitude the largest earthquakes are located offshore the province of Jiangsu, approximately 150 km north of Shanghai municipality. There is a dense cluster of earthquake epicentres from approximately 32.3–34.0°N by 121–122°E. Within this area of high seismicity (and short recurrence intervals), is the highest magnitude earthquake recorded within the catalogue, with a surface-wave magnitude of 7.0. On 21 May 1984 a 6.3 M_s event below the South Yellow sea was felt in nearby coastal communities and also northern Shanghai [4]. To the west of the described area in mid Jiangsu and the western part of Shanghai municipality is further high seismicity but with lower magnitudes. Within Shanghai municipality the largest magnitude earthquake occurred in Nanhui County on 1 September 1624 with a magnitude of 4.8.

A further cluster of high magnitude epicentres (greater than or equal to 5.0) are identified to the west of Shanghai municipality in south and southwestern Jiangsu. The Liyang earthquakes of 1974 and 1979 (5.5 M_s and 6.0 M_s), 225 km west of Shanghai, are exceptional recent evidence of damage within an area considered to be of low hazard [5,6] with a maximum intensity of VII and VIII for the two earthquakes, respectively [7]. The 1974 earthquake killed eight people and there were 214 injured. In all, 11,081 houses were destroyed and 21,709 damaged. The 1979 earthquake, which was within 20 km of the 1974 event, resulted in 41 fatalities, 3000 injuries, 113,909 collapsed houses and 272,000 homes damaged [6]. East of Shanghai there is low seismicity with isolated earthquakes in all

magnitude bands up to 6.0–6.9. Seismicity is low elsewhere within the area especially in Anhui and southern Zhejiang. The area of hazard assessment is chosen as 29–34°N and 118–124°E. Within this zone there are 1165 events (97.1% of total).

4. Seismic hazard

The extreme distributions of Gumbel [8] are evaluated to determine the peak ground acceleration and intensity for the 90% probability of non-exceedance in 50 years (475-year return period) and 99% probability of non-exceedance in 50 years together with the 25, 50 and 100 years estimations. This seismogenic free-zone method, independent of any Euclidean zoning assumptions, has been applied in various parts of the world [9,10].

4.1. Peak ground acceleration

Gumbel's [8] first distribution is used to estimate PGA. It is unlimited (has no upper bound) and is of the form

$$GI(a) = \exp\{-\exp[-\alpha(a-u)]\}, \quad (1)$$

where a is extreme PGA value for a selected time interval, u is the characteristic modal value and α a further parameter. $GI(a)$ is the probability that a is an extreme of PGA at a point. An attenuation law applicable to the region is used to determine values of a from each earthquake magnitude. Extreme values of a are then extracted from a predefined extreme time interval and input into a linear form of Eq. (1) through which PGA, in cm s^{-2} , is determined for

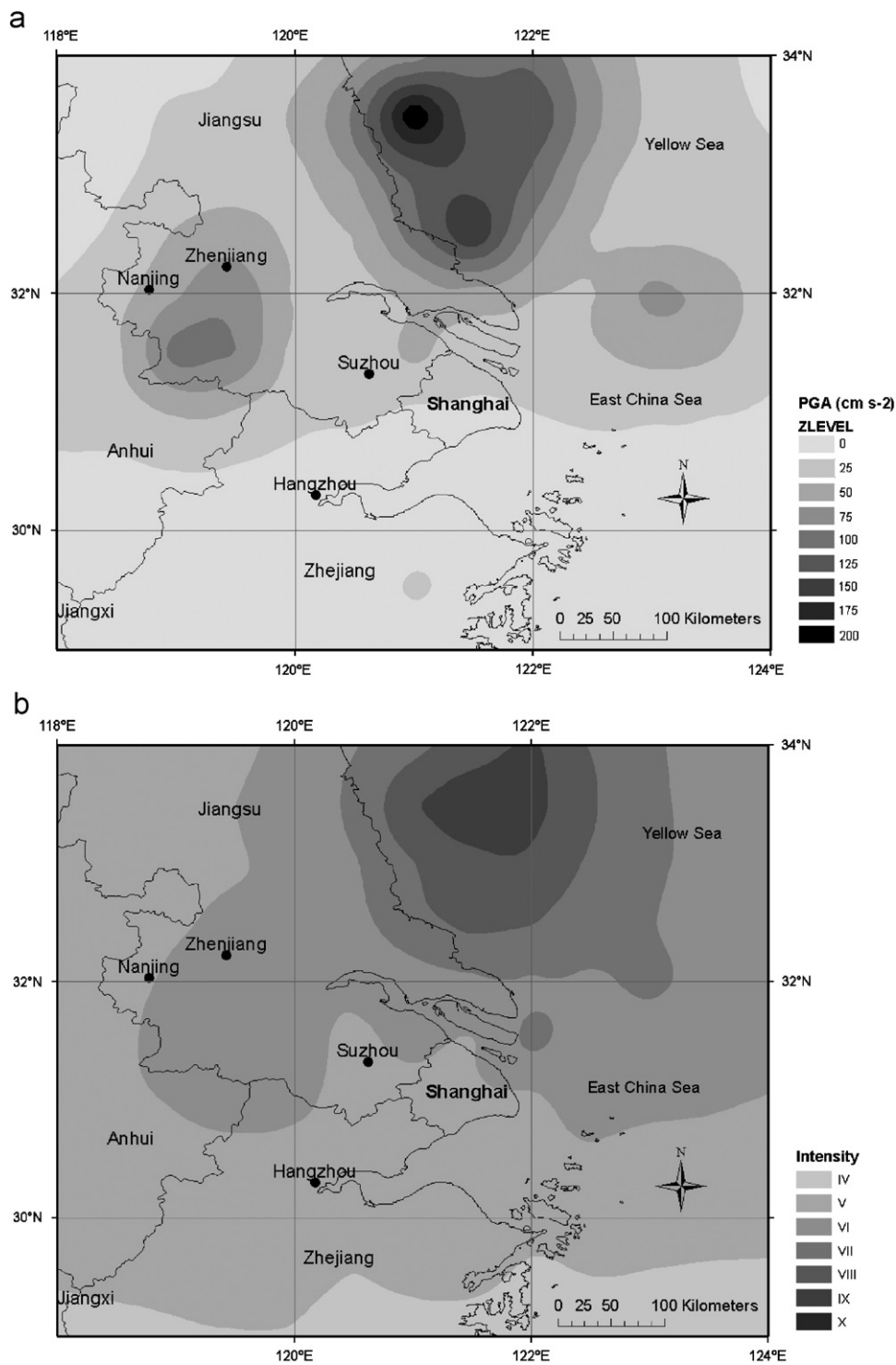


Fig. 3. (a) The peak ground acceleration with 90% probability of non-exceedance in 50 years for Shanghai and its vicinity from Gumbel I method. Values are in cm s^{-2} . Extreme interval is 3 years. Period of catalogue 1905–2004 with threshold magnitude of 4.0 for bedrock site. (b) The maximum intensity with 90% probability of non-exceedance in 50 years from Gumbel III method. Extreme interval is 3 years. Period of catalogue 1905–2004 with threshold magnitude of 4.0. Intensity scale is the Chinese Intensity Scale as defined in Table 2.

varying probabilities and time periods [10]. The choice of attenuation law is from SSB [11,12].

$$\log \text{PGA} = 1.3012 + 0.6057M_s - 1.7216 \log(R + 1.126 \exp(0.482M_s)), \quad (2)$$

where M_s is surface-wave magnitude and R is hypocentral distance in km.

Analysis of completeness from cumulative frequency plots indicates that the catalogue is complete for magnitudes equal or greater to 4.0 from 1905. For records in the

Table 1
PGA (cm s^{-2}) and maximum intensity for Shanghai city with 90% and 99% probability of non-exceedance (pnbe) in 50 years and 25, 50 and 100 year values

Shanghai: 31.14°N 121.29°E	90%pnbe 50years	25 years	50 years	100 years	99%pnbe 50years
PGA	25.0	13.8	16.4	19.1	48.7
Intensity	VI	V	V	VI	VII

Intensity scale is the Chinese Intensity Scale as defined in Table 2.

catalogue that do not contain a focal depth value, a mid-crustal value of 15 km is assumed. A 2.5° cell with 0.5° overlap strategy is used to map and contour the 90% probability of non-exceedance in 50 years (Fig. 3a) and tabulate the 25, 50, and 100 years PGA for Shanghai (Table 1).

4.2. Intensity

Gumbel's [8] third asymptotic distribution is used to estimate intensity. It is upper bounded and of the form

$$\text{GIII}(m) = \exp\left[-\left(\frac{\omega - m}{\omega - u}\right)^k\right], \quad (3)$$

where m is the maximum or extreme magnitude for a selected time interval, ω is the upper bound magnitude parameter, u the characteristic extreme value and k related to the curvature of the distribution. The evaluation of Gumbel's third distribution has been used widely to determine extreme magnitude [9,13] because of the physical realistic upper bound at higher magnitudes. The fact that there is a finite limit to the build up of strain energy is an inescapable physical reality [14]. A similar analogy can be stated for earthquake intensity. The Chinese seismic intensity scale is similar to Modified Mercalli which has a maximum intensity value of XII. The upper bounded third distribution of Gumbel would again provide a mathematical boundary to a limited physical scalar. A non-linear least squares method is applied to estimate the parameters ω , u and $1/k$. Makropoulos and Burton [15] produce a comprehensive account of the mathematical procedure. For the Shanghai region and its vicinity the following intensity–magnitude relation is applied [12].

$$I = 3.5751 + 1.2972M_s - 3.0988 \log(R + 15), \quad (4)$$

where I is intensity on the Chinese Intensity Scale, M_s is surface-wave magnitude, and R is hypocentral distance in km.

A 2.5° cell with 0.5° overlap is employed to map, contour (Fig. 3b) and tabulate (Table 1) the maximum intensity for the same probabilities and time periods as with the PGA analysis. A 3-year extreme interval allows a Gumbel III distribution to be drawn in the most cells possible.

These contoured maps illustrate localised areas of relatively higher and lower seismic hazard. There are three distinct areas of higher hazard within this area. The broadest is offshore and adjacent to southern Jiangsu. Within this $1.5^\circ \times 1.5^\circ$ section, PGA values for a typical

bedrock site, are in the range $100\text{--}150 \text{ cm s}^{-2}$, for a 90% probability of non-exceedance in a 50-year period. The corresponding maximum intensity is VII. A further offshore higher hazard section is identified southeast of the coastal-offshore Jiangsu region, at over 75 cm s^{-2} . These localised sections of increased seismic hazard are associated with continental shelf basins, in specific the Neocathaysian massif which separates the Yellow and East China seas and is the result of mid to late Mesozoic rifting [3]. This area of higher seismic hazard is termed the southern Yellow Sea Seismic Zone [16]. A third section of PGA values of over 100 cm s^{-2} , and corresponding maximum intensity VII is identified in southwestern Jiangsu, to the south of the settlements of Nanjing and Zhenjiang. This is known as the downstream Yangtze River Seismic Zone and associated with tertiary rifts and the north Jiangsu basin, which has a heat flow higher than the average value for the South China Block [16]. Seismic activity within the three described zones is a result of reactivation of ancient zones of weakness [17]. In general, most earthquakes within the Shanghai area and its vicinity are on or near faults formed in former tectonic environments. Juan [3] acknowledges that subduction of the Philippine and Pacific plates under the Eurasian plate and associated asthenosphere upwelling is a mechanism for potential rifting. However, this influence is limited and although variations in seismic hazard can be observed the overall seismic hazard in Shanghai and its vicinity is low. The PGA results are comparable to results from GSHAP [18]. The primary reason for low to medium hazard in this area of China (as opposed to high hazard in the west) is that southeastern China lies in a stress-shadow from the thrust of the India–Eurasia collision, protected by the Sichuan mantle uplift and North-South Seismic Zone to the west [19]. Furthermore, major tectonic features are orthogonal to this principal stress with predominantly strike-slip and normal faulting in a northeasterly orientation [20]. However, the minority of faults which are striking in a northwestern direction have been reactivated in geologically recent times. This has resulted in earthquakes occurring where these two perpendicular striking faults cross, e.g. Liyang.

Table 1 tabulates the PGA and maximum intensity for Shanghai city. With a value of 25 cm s^{-2} , for a 90% probability of non-exceedance in a 50-year period (1 in 10 chance of exceedance in 50 years), it can be stated that seismic hazard for the city is low to medium. By considering the 99% probability of non-exceedance in a

Table 2
The Chinese Intensity Scale from Ref. [34]

Intensity grade	Perception of people	Other phenomena effects
I	Not felt	
II	The tremor is felt only in isolated instances of individuals at rest and indoors	
III	Felt indoors by few people at rest	Doors and windows rattle slightly; Hanging objects swing slightly
IV	Felt indoors by many and felt outdoors by very few. A few people are awakened	Doors and windows rattle; Hanging objectives swing obviously. China, glass and other objects rattle
V	The earthquake is felt indoors by most, outdoors by few. Many sleeping people awake	Doors, windows and roofs tremble and rattle. Small pieces of plaster fall. Hairline cracks in the plaster of walls. Some tiles fall from the eaves. Very few bricks from roofs and chimneys fall; unstable objects swing
VI	Most people lose their balance, a few people are frightened and run outdoors	Damage — cracks appear in the walls, tiles fall from eaves, a few roofs or chimneys fracture or fall; cracks appear in river banks and soft earth. Sand boils and water spouts in saturated sand layers. Slight cracks in some independent chimneys
VII	Most people are frightened and run outdoors. The earthquake is felt by bicycle riders and car drivers	Slightly damaging — some parts of houses damaged and cracked. No need for repair or slight need to repair. The building can be continued to be used after the repair; landslips occur in river banks. Sand boils and water spouts frequently in saturated sand layers. Many cracks occur in soft earth. Most independent chimneys damaged
VIII	Most persons find it difficult to stand and to move	Moderately damaging – structural damage and the buildings need to be repaired to be used; cracks also occur in the hard dry earth. Most independent chimneys damaged heavily. Tops of trees break. Some people and animals injured and even death due to building damage
IX	People may be forcibly thrown to the ground when they move	Heavily damaging — buildings suffer heavy structural damage. Some parts collapse. It is difficult to be repaired; many places of the dry hard earth have cracks. Bedrocks may have fractures and slips. Landslides occur very often. Most independent chimneys collapse
X	Bicycle riders will be forcibly thrown to the ground. People who are in unstable state will be thrown from their position and they will feel as if they have been thrown upwards	Most buildings collapse; landslides in mountain regions. Seismic faults created. Arch bridges on bedrock damaged. Most independent chimneys damaged from the base or collapse
XI		Almost all buildings collapse; very long seismic faults extended. Many landslips and mountain collapse
XII		Earth surfaces change radically. Landscape greatly changed

50-year period (1 in 100 chance of exceedance in 50 years) the PGA value is just below 50 cm s^{-2} . Importantly though the intensity value is VII. With the existence of the Yellow Sea Seismic Zone, the downstream Yangtze River Seismic Zone and the fact that seismic hazard is enhanced by low attenuation of seismic waves in a stable continental region [21,22] attention is required in terms of potential damage in Shanghai and its urban settlement. The nearby Liyang events are recent modern day evidence of intraplate earthquake damage. The necessity to estimate potential damage for a mega-city within a low to moderate seismic hazard region will have more impact in terms of economic and infrastructure losses than that of a higher hazard region and lower population density. With an alternative method of determining hazard for example compared to [23,24] through extreme value statistics, the seismic vulnerability and consequential seismic risk can be estimated.

5. Seismic risk and estimation of expected building damage

Seismic risk in its simplest terms can be expressed as the product of seismic hazard and seismic vulnerability or exposure. Types of vulnerable structures [25] can include

lifeline systems (railways, bridges), critical complexes (hospitals, nuclear power plants, airports) and individual buildings of various types (commercial, residential and industrial).

The Seismic Risk Group at the University of East Anglia (UEA) with the Shanghai Seismological Bureau (SSB) have investigated potential building damage for Shanghai within a GIS environment [26]. A combination of street maps, fault database and building stock data have been collated for mapping and analytical purposes. Building inventory data provides information on the address, the type of building structure, number of storeys, floor area summed over the number of storeys in m^2 and age of building. In this investigation the potential building damage is determined for three representative districts of metropolitan Shanghai: Putuo, Nanjing Road and Pudong (Figs. 4–7).

5.1. Putuo

This district of western Shanghai city centre is part of Puxi and has an area of 55 km^2 and is considered to be a traditional urban dwelling area.

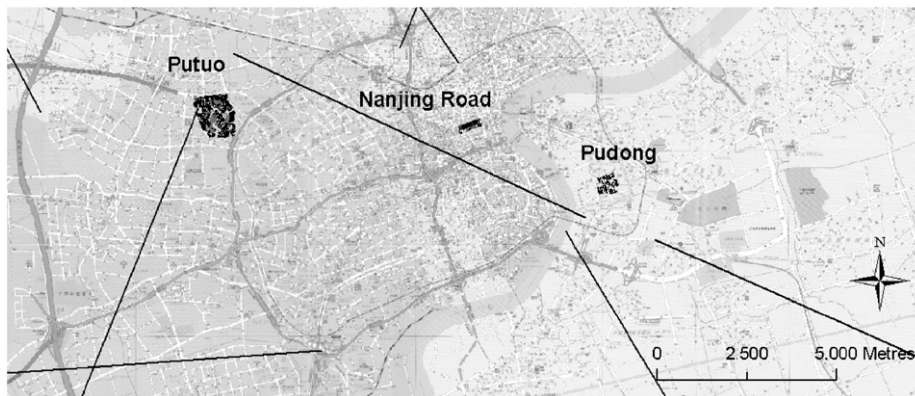


Fig. 4. Shanghai city centre and location of Putuo, Nanjing Road and Pudong building stock. Dark lines are location of known faults.

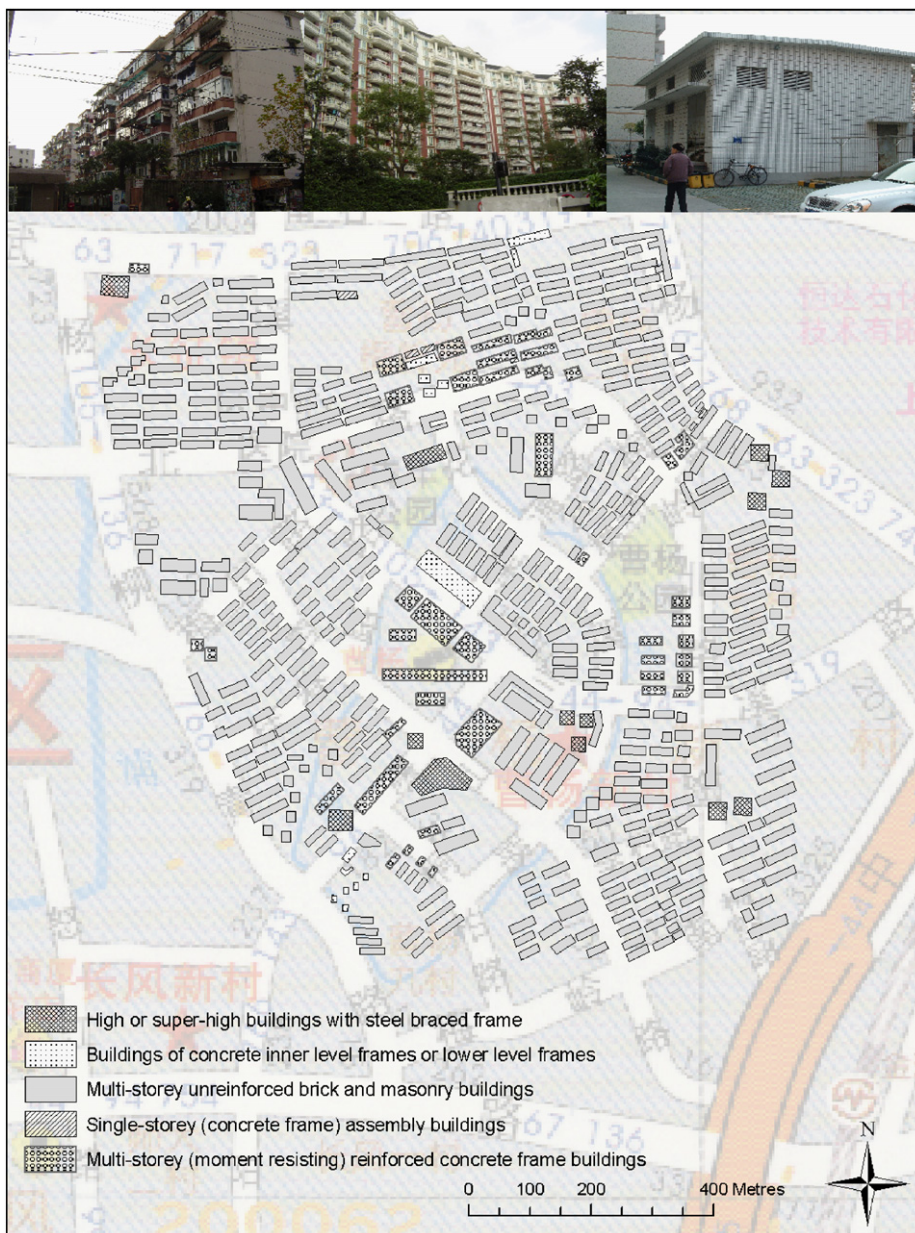


Fig. 5. Putuo building stock. Illustrations show examples of randomly selected building types. From left to right these are multi-storey unreinforced brick and masonry buildings, multi-storey (moment resisting) reinforced concrete frame building and single-storey (concrete frame) assembly buildings. Sample building stock [26] provided by SSB. The road crossing north of the buildings is called Wuning Road.

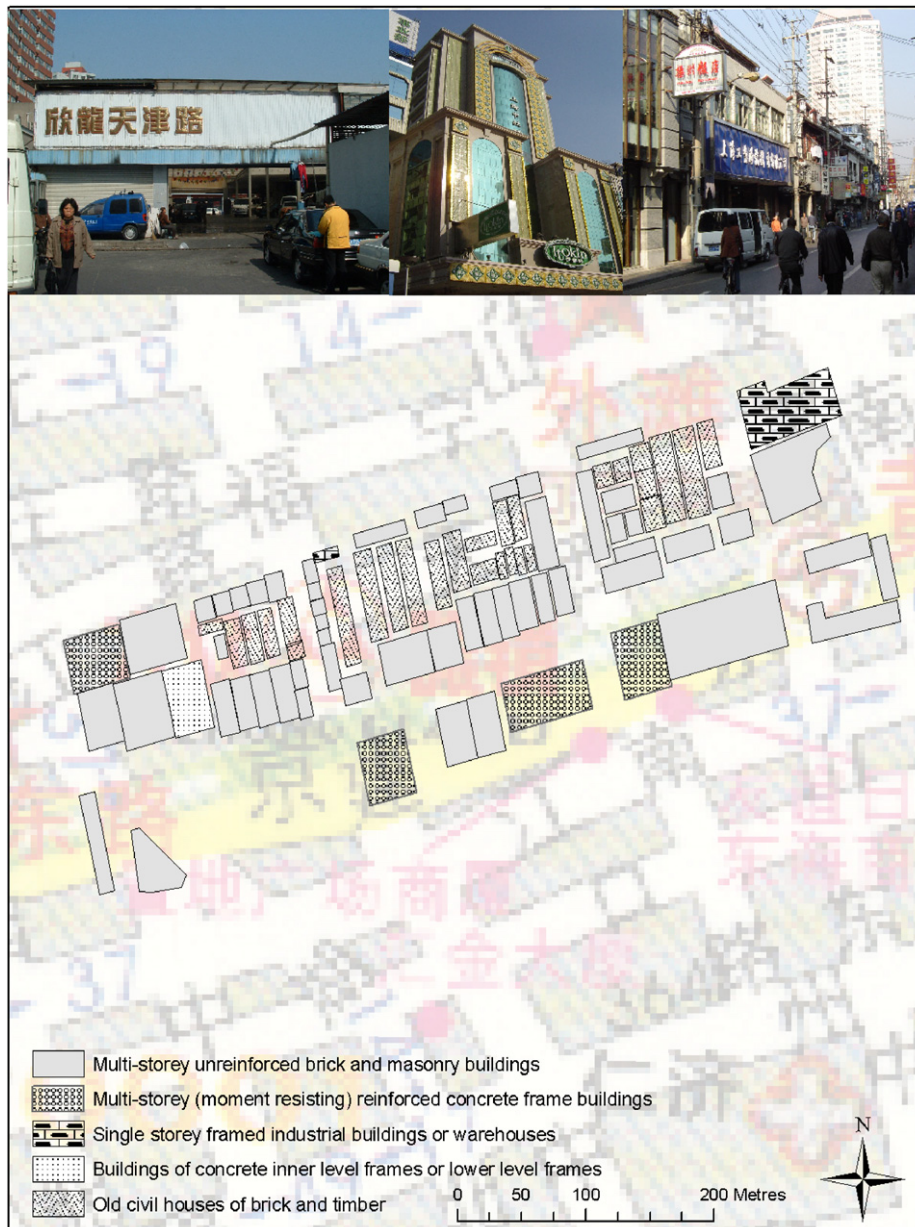


Fig. 6. Nanjing Road building stock. Illustrations show examples of randomly selected building types. From left to right these are industrial buildings or warehouse with single-storey, building of concrete inner level frames or lower level frames and old civil houses of brick and timber. Sample building stock [26] provided by SSB. The road passing between the buildings is called Nanjing Road East.

5.2. Nanjing Road

As part of the Huangpu district, Nanjing Road is known as cosmopolitan area of the city famous for large-scale commercial outlets including “western” style buildings.

5.3. Pudong

Pudong district, covering 522 km², lies east of the Huangpu River and is at the centre of Shanghai’s recent economic boom. In 1990 the Chinese central government set up a special economic zone within this district including constructing high-rise buildings, offices and the main

central business district called Lujiazui. This financial district includes the high-rise construction of the Jin Mao tower, with a height of 421 m, which is built to withstand typhoon winds and earthquakes to magnitude 7 [27]. However, Pudong is generally a mixture of newly constructed multi-storey buildings, built within the last 10 years and poorly maintained dwellings constructed of brick, masonry and timber over 30 years old.

Table 3 shows the building type and construction description and Tables 4 and 5 show the number, and floor area (m²) of buildings in the survey for the three districts of Shanghai. There are a total of 791 buildings for this survey divided into seven unique building types.



Fig. 7. Pudong building stock. Illustration shows an example of a high or super-high building with steel braced frame. Sample building stock [26] provided by SSB. The road crossing north of the buildings is called Weifang Road.

The survey area with the highest number of buildings is Putuo with 543 (68.6% of total), followed by Pudong with 158 (20.0%) and Nanjing Road with 90 (11.4%). The main building type is multi-storey unreinforced brick and masonry buildings (85.8%) and in contrast there are only two (0.3%) single-storey framed industrial buildings or warehouses in this survey. In Putuo and Nanjing Road, five of the seven building types are represented with only two of the seven types in Pudong (multi-storey unreinforced brick and masonry buildings and high–super-high multi-storey buildings). 65.3% of the total floor area of the building stock is for Putuo, with 16.7% and 18.0% in Nanjing Road and Pudong, respectively. Figs. 4–7 show the location and distribution of building types for the three

areas together with photographic examples of the seven building types.

Potential building damage can be estimated by considering the probability of damage in terms of a specific damage grade or damage state. In the Chinese classification system [28] there are five damage states (Table 6) similar to the EMS98 classification. These are: generally no damage (D1), mild damage (D2), moderate damage (D3), serious damage (D4) and total destruction (D5).

For a particular building structure type the Mean Damage Factor can be expressed as

$$\text{MDF}_1 = \sum_{\text{DS}} (P_{\text{DSI}})(\text{CDF}_{\text{DS}}). \quad (5)$$

Table 3
Classification and description of the seven building types from three independent districts of Shanghai city for building damage estimation

Building type	Description of construction	Dates of construction	Number of storeys	Occupancy type
Multi-storey unreinforced brick and masonry buildings	Built of bricks consisting of either clay bricks, fine coal ash bricks or small hollow laying blocks (cement)	1950–2003	1–8	Residential/commercial
Multi-storey (moment resisting) reinforced concrete frame buildings	Constructed of moment resisting frame with reinforced concrete pillars and beams	1970–2003	1–30	Residential/commercial
Single-storey framed industrial buildings or warehouses	Industrial buildings or warehouses built with concrete pillars, brick pillars, steel pillars or a mixture of pillars	1970–1980	1	Industrial
Buildings of concrete inner level frames or lower level frames	Buildings consisting of inner concrete frames and outer brick walls and pillars/multi-storey buildings of bricks consisting of bottom concrete frames	1974–1998	10	Residential/commercial
Single-storey (concrete frame) assembly buildings	Public buildings such as cinemas, theatres, clubs and lecture halls constructed of a single-storey concrete frame	1957–1999	1	Commercial
Old civil houses of brick and timber	Unreinforced brick masonry, stone or timber urban buildings	< 1960	2–5	Residential
High or super-high buildings with steel braced frame	Modern multi-level engineered buildings with steel moment resisting frame	> 1990	> 20	Residential

Table 4
Number and type of building from three independent districts of Shanghai city for building damage estimation

Building type	Putuo	Nanjing Road	Pudong	Total
Multi-storey unreinforced brick and masonry buildings	468	55	156	679
Multi-storey (moment resisting) reinforced concrete frame buildings	43	4	0	47
Single-storey framed industrial buildings/warehouses	0	2	0	2
Buildings of concrete inner level frames or lower level frames	14	1	0	15
Single-storey (concrete frame) assembly buildings	5	0	0	5
Old civil houses of brick and timber	0	28	0	28
High or super-high buildings with steel braced frame	13	0	2	15
Total number of buildings in survey	543	90	158	791

Table 5
Floor area (m²) for three independent districts of Shanghai city for building damage estimation

Building type	Putuo	Nanjing Road	Pudong	Total
Multi-storey unreinforced brick and masonry buildings	945,428	190,436	327,418	1,463,282
Multi-storey (moment resisting) reinforced concrete frame buildings	166,456	99,310	0	265,766
Single-storey framed industrial buildings/warehouses	0	1880	0	1880
Buildings of concrete inner level frames or lower level frames	57,821	9000	0	66,821
Single-storey (concrete frame) assembly buildings	688	0	0	688
Old civil houses of brick and timber	0	33,612	0	33,612
High or super-high buildings with steel braced frame	135,341	0	31,806	167,147
Total floor area (m ²) for buildings in survey	1,305,734	334,238	359,224	1,999,196

Here MDF_1 is the mean damage factor for given earthquake intensity, DS is damage state, P_{DSI} is the probability of damage state DS at intensity I, and CDF_{DS} is the central damage factor for a given damage state. The central damage factor is determined from the range of damage factor probabilities at a particular damage state. In this paper, the central damage values of Chen et al. [29] are used. Fig. 8

presents the MDF as a function of intensity for the seven building types based on data supplied by the SSB [26].

The building types can be divided into three distinct categories which are approximate to use in the MSK [30] and EMS vulnerability-intensity scales [31]. The upper curve in Fig. 8 represents the most vulnerable structures which are old civil houses of brick and timber akin to type A of

Table 6
Description of earthquake damage state or grade adopted by Yin [28] and corresponding damage factor values by Chen et al. [29]

Damage state or grade, DS	Range of damage factor (%)	Central damage factor (%)	Description
Grade 5: Total destruction	70–100	85	General structure of building has already collapsed or is on the verge of collapse, in an unreparable state. The building has lost all its original structural integrity. Most components of a building have very serious damage or serious damage.
Grade 4: Serious damage	40–70	55	Building is difficult to repair. Most components of the building are damaged at serious damage. A few components are damaged below this level.
Grade 3: Moderate damage	10–40	25	The building structure could return to its original form after some repairs. Part of the components of a building are moderately damaged, a few components are seriously damaged.
Grade 2: Mild damage	5–10	8	Structure only needs simple repairs to return to its original form. Partially damaged components of the building belong to mild level damage; a few of the components are at the moderate damage level.
Grade 1: Generally no damage	0	0	No repairs needed. Most components are not damaged. Only a few are mildly damaged.

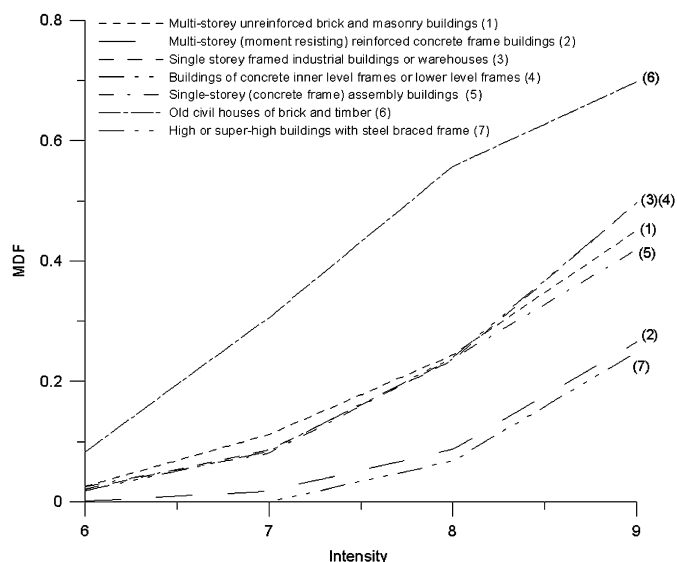


Fig. 8. Mean damage factor as a function of intensity for seven building structure types in Shanghai based on data supplied by the SSB.

MSK/EMS. The lower two lines signify the least vulnerable structures of multi-storey (moment resisting) reinforced concrete frame buildings and high–super-high multi-storey building or type C on MSK and even earthquake engineered types D and beyond on EMS. The four remaining building structure types are similar to type B.

Earthquake intensity scales are based on a long history of documented and observed effects of earthquakes at multiple sites. This information rates the degree of damage to buildings and is used as a way of classifying earthquake damage to “non-engineered” buildings of little or no seismic resistance. For buildings with engineered aseismic design, representative of the higher categories of EMS98, loss models are not found from traditional intensity ratings but derived from instrumental response spectra and in particular spectral displacement [32]. However, because

anti-seismic designed buildings have not yet been exposed to recent earthquakes within this region and the current lack of displacement spectra information, it is not possible to deduce loss estimation based on spectral displacement models alone for all of the available building stock. Within the Shanghai survey many of the buildings are non-engineered, constructed without building codes, and the Chinese Intensity Scale is therefore the basis from which probable damage is calculated.

Estimation of potential building damage is achieved from MDF values for the seven building structure types at intensity levels determined from the hazard analysis. A maximum intensity of VI, for 90% probability of non-exceedance in 50 years, is determined for Shanghai city from extreme value methods (Table 1). The China Earthquake Administration (CEA) has determined an intensity of VI for Shanghai city again at 90% probability of non-exceedance in 50 years [33]. Using the probabilistic methods of Cornell [23], the SSB propose intensity VII, for 1 in 10 chance of exceedance in 50 years, for Shanghai (personal correspondence). In addition, the extreme value methods also reveal an intensity value of VII at 99% probability of non-exceedance in 50 years. Therefore, the MDF data for intensities VI and VII are utilised. The mean damage factor gives the probability of damage for a particular building type at a specified intensity. However, this value alone does not quantify the quantity of damage at the five damage grades. The SSB have developed damage probability matrices derived from historical studies of earthquake damage within China to quantify how associated damage grades contribute to the MDF value. Consider Table 7 which tabulates the MDF for each building type and associated damage grade levels for the building stock data at intensity VI.

As an example, for multi-storey unreinforced brick and masonry buildings the MDF is 0.02570. That is, as a mean figure, 2.57% of this building type is damaged at intensity

Table 7

Mean damage factor and associated levels of damage at five damage grades for the seven building types at intensity VI

	D1	D2	D3	D4	D5	MDF
Multi-storey unreinforced brick and masonry buildings	0.0000	0.0132	0.0125	0.0000	0.0000	0.02570
Multi-storey (moment resisting) reinforced concrete frame buildings	0.0000	0.0008	0.0000	0.0000	0.0000	0.00080
Single-storey framed industrial buildings/warehouses	0.0000	0.0166	0.0048	0.0000	0.0000	0.02131
Buildings of concrete inner level frames or lower level frames	0.0000	0.0133	0.0055	0.0000	0.0000	0.01878
Single-storey (concrete frame) assembly buildings	0.0000	0.0178	0.0078	0.0000	0.0000	0.02559
Old civil houses of brick and timber	0.0000	0.0437	0.0220	0.0172	0.0000	0.08281
High or super-high buildings with steel braced frame	0.0000	0.0000	0.0000	0.0000	0.0000	0.00000

Summation of D1 through to D5 results in the mean damage factor [26].

Table 8

Mean damage factor and associated levels of damage at five damage grades for the seven buildings types at intensity VII

	D1	D2	D3	D4	D5	MDF
Multi-storey unreinforced brick and masonry buildings	0.0000	0.0337	0.0695	0.0088	0.0000	0.11198
Multi-storey (moment resisting) reinforced concrete frame buildings	0.0000	0.0119	0.0063	0.0000	0.0000	0.01817
Single-storey framed industrial buildings/warehouses	0.0000	0.0475	0.0320	0.0066	0.0000	0.08612
Buildings of concrete inner level frames or lower level frames	0.0000	0.0501	0.0220	0.0121	0.0000	0.08418
Single-storey (concrete frame) assembly buildings	0.0000	0.0466	0.0260	0.0083	0.0000	0.08081
Old civil houses of brick and timber	0.0000	0.0196	0.0871	0.1239	0.0752	0.30585
High or super-high buildings with steel braced frame	0.0000	0.0000	0.0000	0.0000	0.0000	0.00000

Summation of D1 through to D5 results in the mean damage factor [26].

VI. The mean amount of damage for each specific damage grade is determined from the product of the probability of damage at a specific damage grade and the central damage factor. In this case the 2.57% of mean damage for multi-storey unreinforced brick and masonry buildings at intensity VI for Putuo can be divided so that 1.32% is at damage grade D2 and 1.25% at D3. The mean floor area damaged is then the product of the damage at a specific damage grade and the total floor area of the specific building type. Again in this example 12,480 m² (0.0132 × 945,428) and 11,818 m² (0.0125 × 945,428) of floor area is damaged at D2 and D3 grades, respectively, for buildings of multi-storey unreinforced brick and masonry buildings as a mean value for Putuo at intensity VI. This method is applied for Putuo, Nanjing Road and Pudong for intensities VI and VII (Tables 7, 8 and Figs. 9–11). The resulting estimates of building damage for the three areas of Shanghai can be summarised as follows (Table 9).

5.4. Putuo

At intensity VI the mean total damage of this area of Putuo is 25,535 km² or 1.9% of the total floor area. Of the damaged area, 52.4% is at damage grade D2 and 47.5% at D3. There is no damage of multi-storey (moment resisting) reinforced concrete frame buildings at D3 at intensity VI. For intensity VII the mean total damage of this area of Putuo is 113,818 km² or 8.7% of the total floor area. 59.8% of this is at D3 with damage to all building types apart from high or super-high buildings with steel braced frame.

0.7% of the total floor area is damaged at D4 (7.9% of damaged area) with multi-storey unreinforced brick and masonry buildings and buildings of concrete inner level frames or lower level frames having the highest damage in terms of floor area at this damage grade.

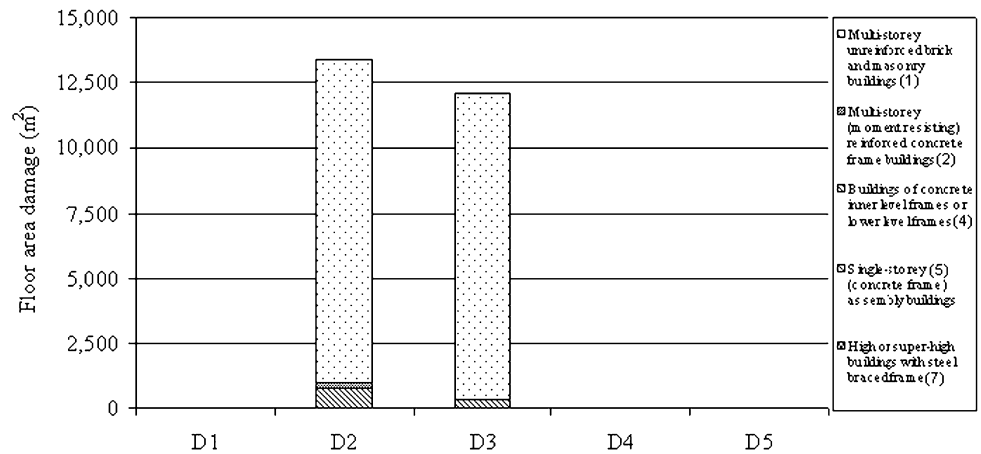
5.5. Nanjing Road

A mean value of 7966 km² or 2.4% of the total floor area is damaged at intensity VI. 52.9% of the damaged area is at damage grade D2 with 39.9% at damage grade D3 and 7.2% at D4. Only old civil houses of brick and timber would suffer damage at grade D4. At intensity VII damage is spread across damage grades D2 to D4 with grade D2 and D3 having the highest proportions with 25.6% and 49.6%, respectively. An important finding is that 7.4% of the damaged area or 0.8% of the total area, as a mean value, will exhibit damage at grade D5. This possible total destruction of buildings is exclusively for the building type of old civil houses of brick and timber. 10.3% of the total floor area is expected to be damaged, as a mean value, at intensity VII for this section of Nanjing Road.

5.6. Pudong

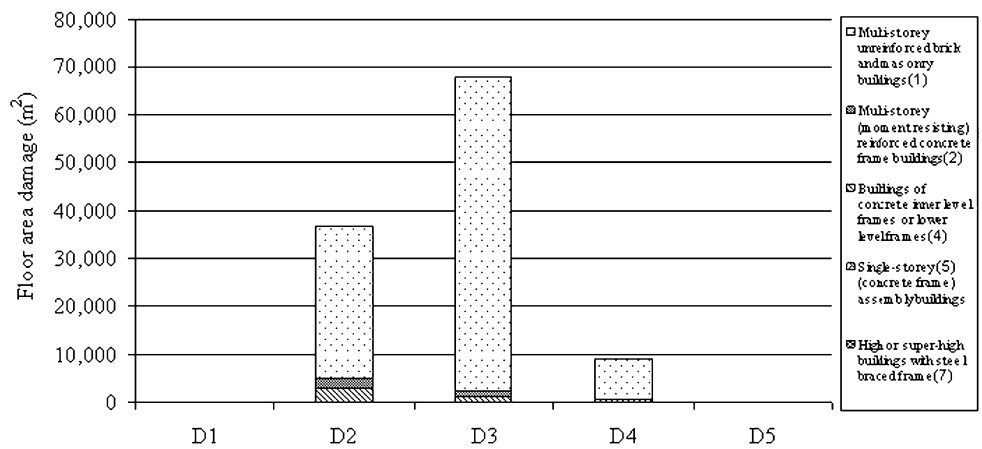
There is no damage for super-high buildings in the Pudong section at intensity VI and VII. At intensity VI damage to buildings of multi-storey unreinforced brick and masonry buildings represents 2.3% of the total area. 51.4% of this damage is at damage grade D2 and 48.6% at D3 with no damage at D4 or D5. At intensity VII damage to

a



Multi-storey unreinforced brick and masonry buildings	0	12,480	11,818	0	0	24,298
Multi-storey (moment resisting) reinforced concrete frame buildings	0	133	0	0	0	133
Buildings of concrete inner level frames or lower level frames	0	788	318	0	0	1,086
Single-storey (concrete frame) assembly buildings	0	12	5	0	0	18
High or super-high buildings with steel braced frame	0	0	0	0	0	0
Totals (m ²)	0	13,393	12,141	0	0	25,535
% of damage area	0.0	52.4	47.5	0.0	0.0	100
% of total floor area	0.0	1.0	0.9	0.0	0.0	1.9

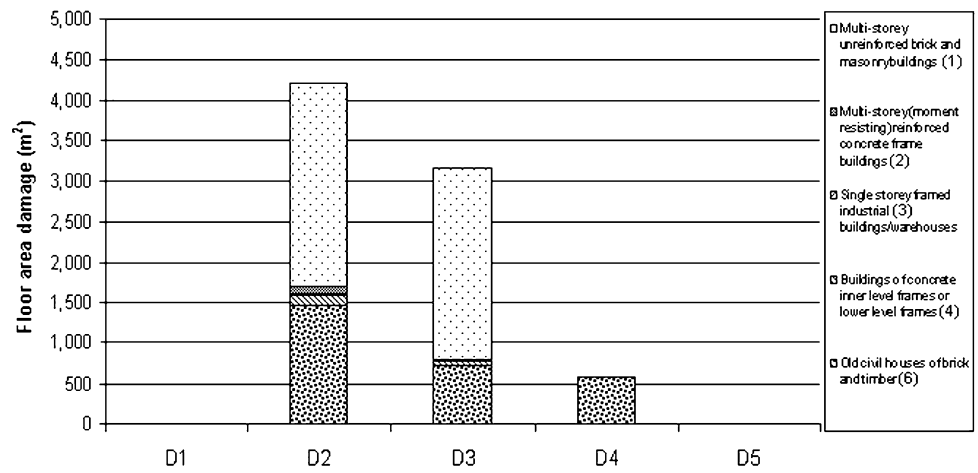
b



Multi-storey unreinforced brick and masonry buildings	0	31,842	65,707	8,320	0	105,869
Multi-storey (moment resisting) reinforced concrete frame buildings	0	1,984	1,040	0	0	3,025
Buildings of concrete inner level frames or lower level frames	0	2,896	1,272	700	0	4,867
Single-storey (concrete frame) assembly buildings	0	32	18	6	0	56
High or super-high buildings with steel braced frame	0	0	0	0	0	0
Totals (m ²)	0	36,754	68,038	9,025	0	113,817
% of damage area	0.0	32.3	59.8	7.9	0.0	100
% of total floor area	0.0	2.8	5.2	0.7	0.0	8.7

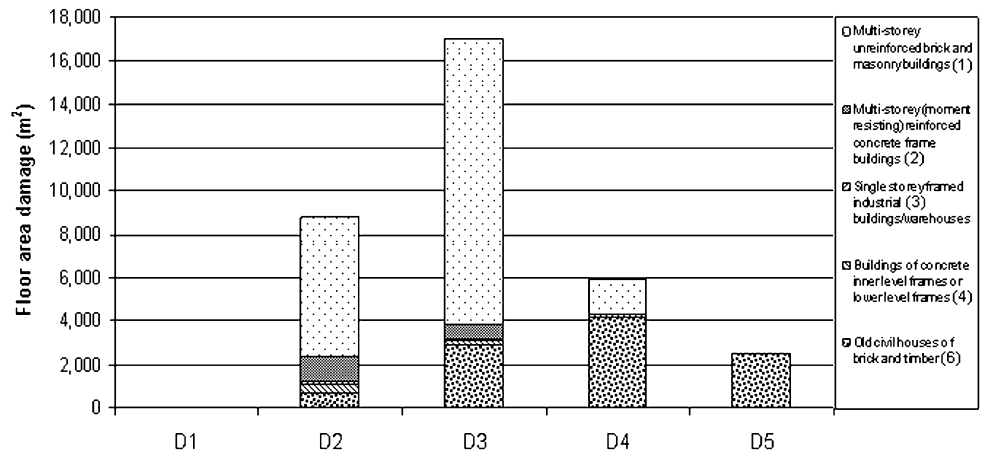
Fig. 9. Probable damage levels in terms of floor area for Putuo building stock at (a) intensity VI and (b) intensity VII.

a



Multi-storey unreinforced brick and masonry buildings	0	2,514	2,380	0	0	4,894
Multi-storey (moment resisting) reinforced concrete frame buildings	0	79	0	0	0	79
Single storey framed industrial buildings/warehouses	0	31	9	0	0	40
Buildings of concrete inner level frames or lower level frames	0	120	50	0	0	169
Old civil houses of brick and timber	0	1,467	738	578	0	2,783
Totals (m ²)	0	4,211	3,177	578	0	7,966
% of damage area	0.0	52.9	39.9	7.2	0.0	100
% of total floor area	0.0	1.3	1.0	0.2	0.0	2.4

b



Multi-storey unreinforced brick and masonry buildings	0	6,414	13,235	1,676	0	21,325
Multi-storey (moment resisting) reinforced concrete frame buildings	0	1,184	621	0	0	1,804
Single storey framed industrial buildings/warehouses	0	89	60	12	0	162
Buildings of concrete inner level frames or lower level frames	0	451	198	109	0	758
Old civil houses of brick and timber	0	658	2,928	4,166	2,529	10,280
Totals (m ²)	0	8,796	17,042	5,963	2,529	34,329
% of damage area	0.0	25.6	49.6	17.4	7.4	100.0
% of total floor area	0.0	2.6	5.1	1.8	0.8	10.3

Fig. 10. Probable damage levels in terms of floor area for Nanjing Road building stock at (a) intensity VI and (b) intensity VII.

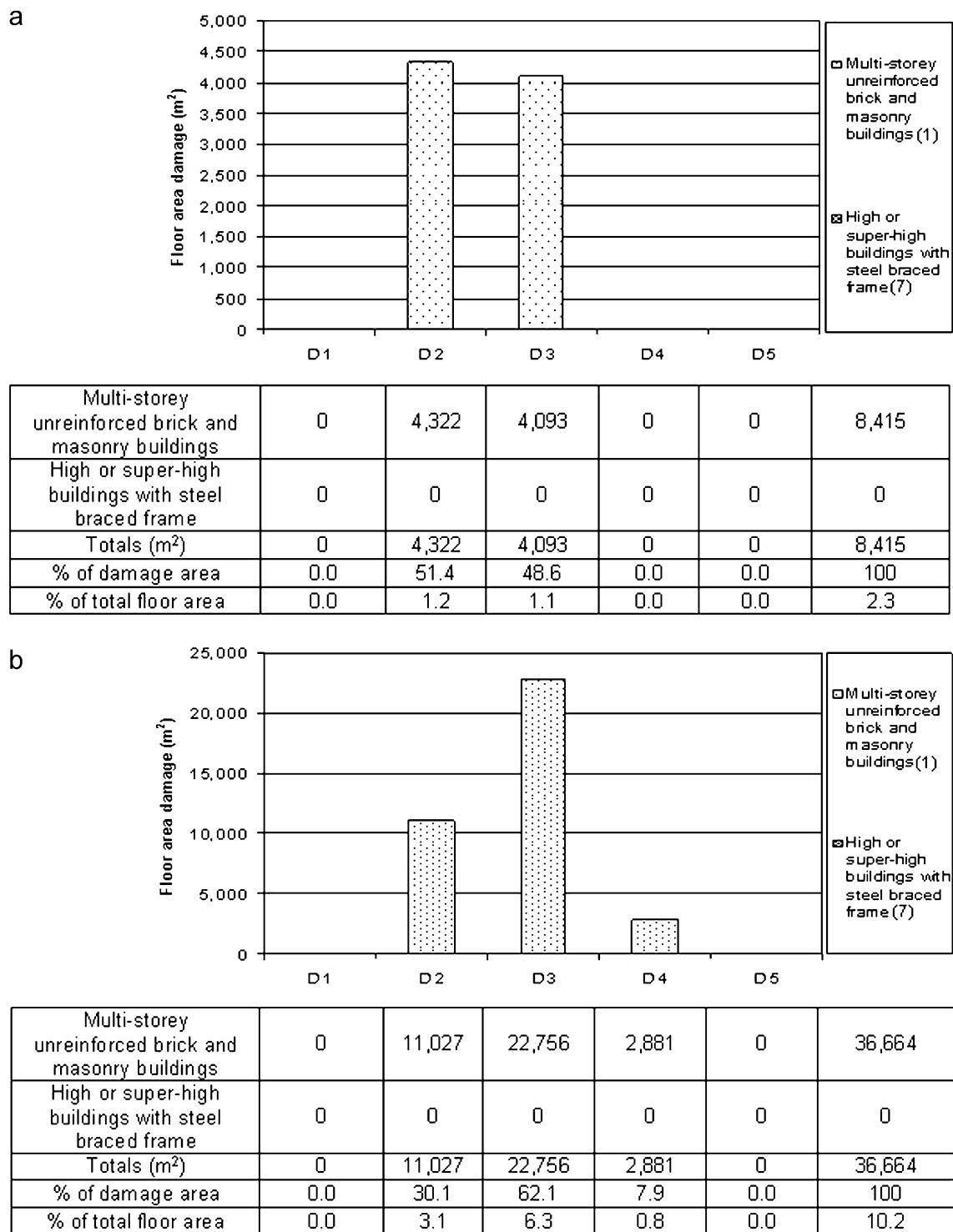


Fig. 11. Probable damage levels in terms of floor area for Pudong building stock at (a) intensity VI and (b) intensity VII.

buildings is 10.2% of the total floor area with 0.8% at damage grade D4. 62.1% of the damaged area is at D3 and 7.9% at D4.

6. Conclusions

Shanghai is an example of a modern day mega-city. Its recent economic, demographic and urban growth has been

rapid and at exceptional levels. This has resulted in contrasting economic and development status between people and property. The increased exposure of the city's infrastructure to natural disasters is evident. This paper has presented an analysis of the seismic hazard and risk in Shanghai and its vicinity from the extreme value distributions of Gumbel. This seismogenic free-zone method determines two zones of higher hazard surrounding the

Table 9
Total probable damage levels for the three areas of Shanghai at intensity VII

	Number of buildings	Floor area (m ²)	D1	D2	D3	D4	D5	Total damage	% of total area
Putuo	543	1,305,734	0	36,754	68,038	9025	0	113,817	8.7
Nanjing Road	90	334,238	0	8796	17,042	5963	2529	34,330	10.3
Pudong	158	359,224	0	11,027	22,756	2881	0	36,664	10.2
Total	791	1,999,196	0	56,577	107,836	17,869	2529	184,811	9.2

Shanghai region termed the Yellow Sea Seismic Zone and downstream Yangtze River Seismic Zone.

In general, the seismic hazard of Shanghai is low to medium with a PGA value of 25 cm s^{-2} for a 90% probability of non-exceedance in 50 years. PGA is a short period ground motion parameter affecting short period structures or low-level buildings. The higher hazard region of the Yellow Sea Seismic Zone, with PGA in excess of 150 cm s^{-2} , could exhibit longer period ground motions and therefore affect higher level buildings within Shanghai. A maximum intensity of VI (for 90% probability of non-exceedance in 50 years) is determined from an extreme value method and also from work published by the CEA. In addition an intensity VII value for Shanghai is found from the extreme value method at 99% probability of non-exceedance in 50 years (and the SSB at 90% probability of non-exceedance in 50 years from an alternative method).

These results are then used to determine potential building damage in three different districts of Shanghai city. The mean damage factor provides an estimation of the average levels of damage for different building structure types determined from damage-vulnerability matrices. Five different building structure types are exhibited in Putuo and Nanjing Road. At intensity VI potential damage within these areas is restricted to the low levels of the damage grade system. However, at intensity VII there is probable significant damage to the most vulnerable buildings of old civil houses of brick and timber at the higher damage grades. Within Pudong these estimations indicate there is no probable damage to high or super-high buildings with steel braced frame at intensity VII.

Acknowledgements

The authors are grateful to Wei Wang, Changqing Cai, Jingyuan Yin and Jianwen Shen of the Shanghai Seismological Bureau who have kindly provided information on Shanghai building stock including photographs and GIS data files. The work was supported in part by the British Council (UK-China Science and Technology Fund). We also thank the reviewers for comments in improving this paper.

References

- [1] Shanghai Municipal Government. <<http://www.shanghai.gov.cn/shanghai/node8059/BasicFacts/index.htm>>, 2006.
- [2] Gu P, Qiu J, Wang Y, Zhang Z. Geology of Shanghai municipality. Geological Atlas of China. Beijing: Geological Publishing House; 2002. p. 173–78.
- [3] Juan VC. Thermal-tectonic evolution of Yellow Sea and East China Sea—implication of transformation of continental to oceanic crust and marginal basin formation. *Tectonophysics* 1986;125:231–44.
- [4] Chung W, Brantley B. The 1984 southern Yellow Sea earthquake of eastern China: source properties and seismotectonic implications for a stable continental area. *Bull Seismol Soc Am* 1989;79:1863–82.
- [5] Chung W, Wei B, Brantley B. Faulting mechanisms of the Liyang, China, Earthquakes of 1974 and 1979 from regional and teleseismic waveforms—evidence of tectonic inversion under a fault-bounded basin. *Bull Seismol Soc Am* 1995;85:560–70.
- [6] Seismological Bureau of Jiangsu Province [SBJP]. Catalog of earthquakes in Jiangsu Province. Beijing: Earthquake Press; 1987. p. 412 (in Chinese).
- [7] Xu S, Liu Y. Similarity of two Liyang earthquakes. *Pure Appl Geophys* 1985;122:894–900.
- [8] Gumbel EJ. Statistics of extremes. New York: Columbia University Press; 1966. 375p.
- [9] Burton PW. Seismic risk in Southern Europe through to India examined using Gumbel's third distribution of extreme values. *Geophys J R Astron Soc* 1979;59:249–80.
- [10] Burton PW, Xu Y, Tselentis GA, Sokos E, Aspinall W. Strong ground acceleration seismic hazard in Greece and neighboring regions. *Soil Dyn Earthquake Eng* 2003;23:159–81.
- [11] Shanghai Seismological Bureau and Tongji University. Seismic zonation by parameters of strong earth movements for Shanghai. Tongji University, 2002 (in Chinese).
- [12] Shi S, Shen J. A study on attenuation relations of strong earth movements in Shanghai and its adjacent area. *Earthquake Res China* 2003;19:315–23 (in Chinese).
- [13] Xu Y, Burton PW, Tselentis GA. Regional seismic hazard for Revithoussa, Greece: an earthquake early warning shield and selection of alert signals. *Nat Hazards Earth Syst Sci* 2003;3:757–76.
- [14] Burton PW. Pathways to seismic hazard evaluation: extreme and characteristic earthquakes in areas of low and high seismicity. *Nat Hazards* 1990;3:275–91.
- [15] Makropoulos KC, Burton PW. Seismic hazard in Greece. I. Magnitude recurrence. *Tectonophysics* 1985;117:205–57.
- [16] Liu L. Stable continental region earthquakes in South China. *Pure Appl Geophys* 2001;158:1583–611.
- [17] Sykes LR. Intraplate seismicity, re-activation of pre-existing zones of weakness, alkaline magmatism, and other tectonism postdating continental fragmentation. *Tectonophysics* 1978;305:371–9.
- [18] Zhang P, Yang Z, Gupta HK, Bhatia SC, Shedlock KM. Global Seismic Hazard Assessment Program (GSHAP) in continental Asia. *Annali di Geofisica* 1999;42:1167–89.
- [19] Molnar P, Tapponnier P. Relation of the tectonics of eastern China to the India–Eurasia collision: application of slip-line field theory to large-scale continental tectonics. *Geology* 1977;5:212–6.
- [20] Zhang Z, Liu C, Wang F. Preliminary study on relation of fault activity and seismicity in Shanghai region. *Earthquake Res China* 2004;20:143–51.

- [21] Mitchell BJ, Pan Y, Chen D, Xie J. Q and crustal evolution in stable continental regions. *Seismol Res Lett* 1993;64:262.
- [22] Nuttli OW. The Mississippi Valley Earthquakes of 1811 and 1812: intensities, ground motion and magnitudes. *Bull Seismol Soc Am* 1973;63:227–48.
- [23] Cornell C. Engineering seismic risk analysis. *Bull Seismol Soc Am* 1968;58:1583–606.
- [24] McGuire RK. FRISK88M: user's manual, version 1.79. Risk Engineering Inc., 4155 Darley Ave., Suite A, Boulder, Colorado, USA; 1996.
- [25] Chen Y, Chen Q, Chen L. Vulnerability analysis and earthquake loss estimate. *Nat Hazards* 2001;23:349–64.
- [26] Xu Y, Burton PW, Cole SW, Cai C, Wang W, Yin J, et al. Seismic vulnerability to three typical regions in Shanghai, China within a Geographical Information System and estimation of expected earthquake losses to buildings. UK/CHINA co-operative report, University of East Anglia, Norwich.
- [27] Korista DS, Sarkisian MP, Abdelrazaq AK, Viswanath HR, Tolloczko JJA, Clarke JN. Design and construction of China's tallest building: The Jin Mao tower, Shanghai. Conquest of vertical space in the 21st century. In: International conference no. 3, London; 1997. p. 289–304.
- [28] Yin Z. Earthquake hazards and prediction for their losses. Beijing: Seismological Press; 1995 (in Chinese).
- [29] Chen Y, Liu J, Chen C, Chen L, Li M. Analysis of earthquake hazards and prediction of seismic risk. Beijing: Seismological Press; 1999 (in Chinese).
- [30] MSK, Report on the Ad-hoc Panel Meeting of Experts on up-dating of the MSK-64 Seismic Intensity Scale, Jena (GDR), 10–14 March 1980, *Gerl. Beitr. Geophys., Leipzig (GDR)* 1980;90(3):261–68.
- [31] Grünthal G, editor. European Macroseismic Scale 1998. Cahiers du Centre Européen de Géodynamique et de Séismologie No. 15. Luxembourg, 1998.
- [32] Calvi GM. A displacement-based approach for vulnerability evaluation of classes of buildings. *J Earthquake Eng* 1999;3:411–38.
- [33] Hu Y. Seismic zoning maps of ground motion parameters. GB 18306-2001 (in Chinese).
- [34] The Chinese intensity scale. Beijing: Chinese standard Press; 1999 (in Chinese).